OPEN ACCESS

International
Journal
Of Modern Engineering Research (IJMER)

Application of a Nanostructured Aluminium Alloy in Internal Combustion Engine Pistons for Mass Reduction

H. Adil[1], S. Gerguri[1], J. Durodola[1], F. Bonatesta[1], F. Audebert[3] F. Saporiti[2]

[1] *School of Engineering, Computing and Mathematics, Oxford Brookes University, Wheatley Campus, OX33 1HX, Oxford, United Kingdom*
[2] *Group of Advanced Materials, Faculty of Engineering, University of Buenos Aires, Paseo Colon 850, Buenos Aires, 1063, Argentina.*
[3] *Department of Materials, University of Oxford, 16 Parks Road, OX1 3PH, Oxford, United Kingdom*
Corresponding Author: H. Adil

ABSTRACT: *The primary focus of this experimental study is to compare the performance of internal combustion engine pistons made of a newly developed nanostructured aluminium alloy (RSA-612) and conventional aluminium alloy 2618. The performance of the new material is based on the ability to reduce piston mass, which is expected to result in reduced piston assembly frictional losses and lead to better engine performance in terms of fuel consumption and power. The new alloy has lower density and higher strength at elevated temperatures than conventional aluminium alloys, making it an ideal piston material in internal combustion (IC) engines. The piston made of the new alloy was 13.5% lighter than the original piston and the engine testing showed that the new alloy could be used in piston applications. The new piston was designed and optimised using finite element analysis. The limited engine testing results presented in this work have shown that the new piston produces enhanced performance in certain operating conditions, whilst performing similarly or slightly worse in others. To ultimately determine whether the new lightweight piston would generate any sizeable difference in engine performance and/or efficiency across the wider engine running envelope, further work is needed.*

KEY WORDS: *Piston, Piston Mass Reduction, Piston Material, Spark Ignition Engine, Nanostructured Aluminium Alloy*

Date of Submission: 14-10-2024 Date of acceptance: 30-10-2024

INTRODUCTION

1.1. Background

The automotive and motorsport industries have been under immense pressure due to emissions control legislations to reduce fuel consumption and alleviate the effects of global warming. Also there is a finite source of hydrocarbon supply which points towards possibility of depletion in the long term [1]. Transport sector especially private transport is the largest contributor to emissions hence improvement in this sector will lead to a bigger reduction in global warming. Emissions reduction is the leading reason to improve engine efficiency. Fuel consumption economy is not only required in transport sector, but also in motor racing since frequent refuelling wastes valuable motor racing time. The time taken for refuelling could be the difference between winning and losing [1].

The automotive industry responded to this challenge with two approaches, which are reducing the overall vehicle mass and improving engine efficiency. Engine efficiency can effectively be enhanced by reducing losses in an engine. Besides thermodynamic losses, mechanical losses also play a significant role and

the majority of these losses are caused by piston assembly [2]. It has been known that piston assembly is responsible for 30–40% [3] or 50% [4] of the frictional losses in an engine.

The piston assembly friction is caused by a phenomenon called piston lateral movement/secondary acceleration. In ideal world, there should be no contact between piston and cylinder wall. However, the conversion of a piston's linear motion into the crankshaft's rotational motion and the piston tilts due to the connecting rod resisting the combustion gas pressure generate force components in the crank mechanism that press the piston against the cylinder wall as illustrated in Fig. 1. This force is generally known as lateral force or connecting rod force, Fig. 2. These forces are responsible for causing friction, engine noise, and reducing this friction can significantly improve engine performance in terms of fuel consumption, torque and power [3].

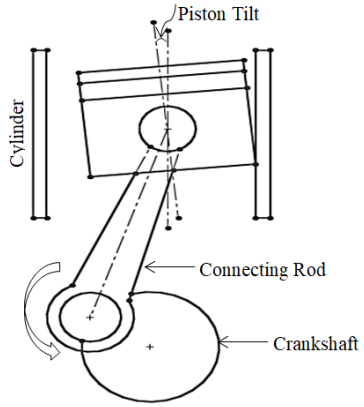

Figure 1: Representative piston tilting motion during an engine operation [3].

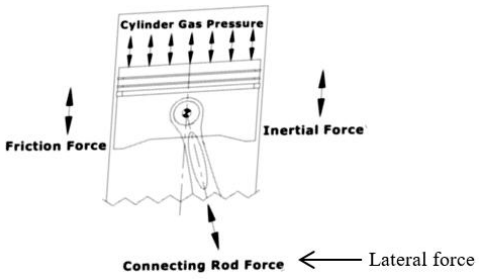

Figure 2: A schematic of different forces acting on a piston of an internal combustion engine [5].

Piston secondary motion also limits the engine rotational speed because the secondary translational and rotational acceleration increases with speed and results in increased secondary inertial forces hence the piston changes direction more frequently and causes the friction to increase [6]. Higher speeds are highly desired in racing to achieving higher accelerations, thus the benefits of lightweight pistons are not only limited to mass produced vehicles.

The lateral force is made of the components of gas and inertial forces [7-8] and the inertial force is dependent on the oscillating mass, hence the lateral force is also dependent on the oscillating mass which can be seen in Eq. (3) in reference [8], also given later in the article as Eq. (3). The oscillating mass includes piston, pin, rings etc. The piston and the piston pin account for the greatest proportion of the oscillating masses. Any weight reduction undertaking must therefore start with these components. This approach is taken in this work using a newly developed aluminium based nanostructured alloy for pistons. Aluminium based nanostructured alloys have microstructure of nanometre sized particles embedded in the aluminium matrix.

1.2. Research Motivation

The motivation for the work presented in this paper is the superior mechanical properties at elevated temperatures exhibited by a newly developed aluminium based nanostructured alloy. The new alloy has lower density and higher strength at elevated temperatures than conventional aluminium alloys, making it an ideal piston material in internal combustion (IC) engines. The improved properties of the new alloy will enable engineers to design lightweight pistons with reduced mass. The aim of this paper is to assess the feasibility of

using this alloy in internal combustion engines' piston applications for mass reduction that will likely reduce piston frictional losses in an engine and lead to improvement in engine's efficiency in terms of fuel consumption, torque and power. It will not only improve engine performance, but will also reduce piston wear therefore improve piston fatigue life and engine reliability [9]. Many researchers such as [10] have studied the effect of piston mass and found that decreasing piston mass decreased the thrust force acting on the liner therefore decreased friction. However; not everyone agrees with this, Goenka and Meenika [11] argue that reduction in friction might be due to the skirt design since mass reduction of piston requires a complete redesign of the piston or piston skirt, but they have not proved this hypothesis. In this work, the piston external envelope and skirt design has been kept unmodified not to affect the combustion characteristic of the engine. In addition to not affecting combustion characteristic of the engine other features shown in Fig. 11 were kept unmodified so the new piston will be compatible with existing engine components.

1.2.1. Application of Nanostructured Aluminium Alloys in Pistons

Earlier engine designers had a limited list of materials to choose from when designing a component; however, that list has grown significantly due to the developments in materials. The materials for piston applications also evolved ever since starting with the cast iron to super alloys in the present [12].

Nanostructured aluminium alloys such as the one investigated in this project can be used in both types of engine, diesel and petrol. Due to higher compression ratios in diesel engines, there are higher demands on mechanical components and tend to be more robust and heavy; therefore, the development of lighter and resistant alloys is also beneficial for those engines. However, the main interest is to use this alloy in Otto cycle/petrol engines because they operate faster than diesel engines and the inertial forces are significantly higher. The inertial forces depend on the speed and mass [8]; the lighter piston will therefore produce greater reduction in inertial forces in petrol engines. In petrol racing engines, the rotational speed can reach values of order of 20000 rpm compared to 6000 rpm limit posed by diesel engines. Furthermore, the trend of changing from diesel to petrol in small high speed engines will further encourage more efforts to be put into developing high temperature aluminium alloys.

Not many researchers seem to have investigated the application of nanostructured aluminium alloys in pistons and in this work only one study found that have tried to apply nanostructured aluminium alloys in piston application [13]. It is not yet known if the project had tested any component for an application demonstration as planned. It was however clear that, the consolidation and extrusion processes needed further optimisation in order to eliminate porosity and improve high temperature properties [13].

The graphs in Figs. 3-4 compare the yield strength and ultimate tensile strength (UTS) values of the new alloy with the existing piston alloy 2618. 2618 is widely used for piston applications in high performance engines. Alloy 2618 is also used in the test engine used for this work. More detailed microstructural characterisation of the new alloy investigated in this work can be found in [14].

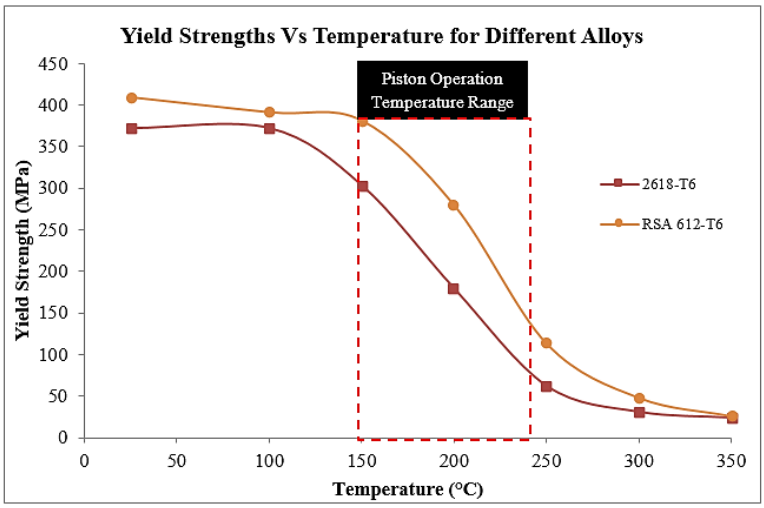

Figure 3: Yield strength comparison of the original and new alloys.

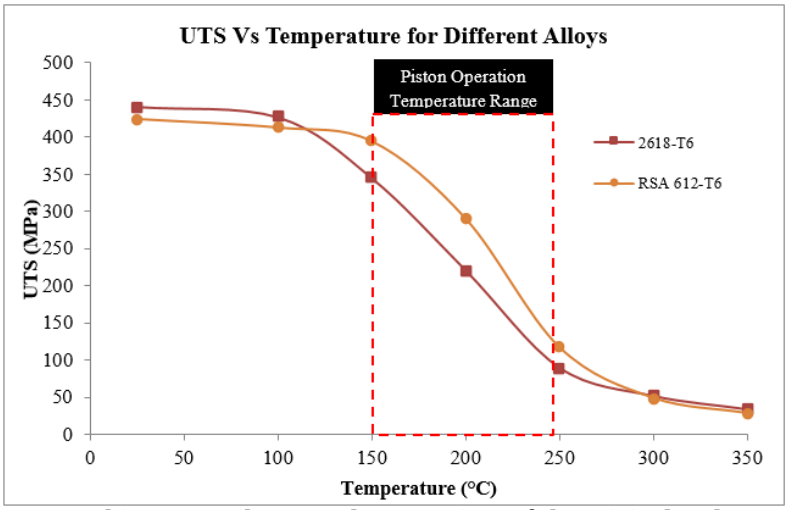

Figure 4: Ultimate tensile strength comparison of the original and new alloys.

About 80% of the piston mass is located in the area from the centre of the piston pin to the upper edge of the crown while the remaining 20% is below the centre of the piston pin to the end of the skirt (Fig. 5a) [15]. The temperature from the centre of the piston pin to the upper edge of the crown could range from 130 °C to 265 °C (in this case) (Fig. 5b). The new alloy has significantly higher strengths in this temperature range (shown in Figs. 3-4) and will enable to reduce piston mass. Furthermore, the new alloy is 7.61% lighter than 2618 (Table 2), the lower density of the new alloy is due to the new alloy having considerable amount of magnesium (13.5 wt%) which is 36% lighter than aluminium and silicon (7 wt%) which is about 17 % lighter than aluminium.

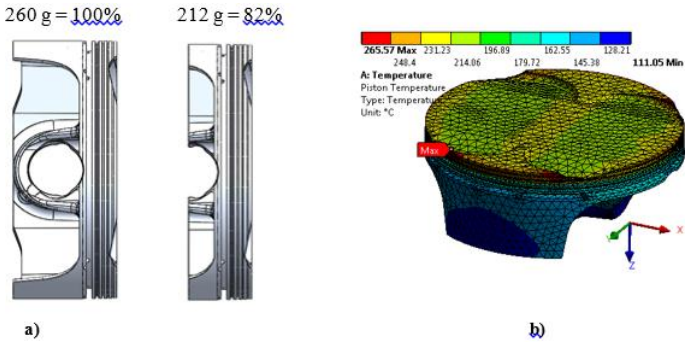

Figure 5: Mass and temperature distributions of KTM 450 XCF piston.

The piston used in this work is from a motorbike engine (2008 KTM 450 XCF) and it was reversed engineered using a laser scanning and other measuring techniques. The load calculations require some engine parameters, which are given in Table 1.

Table 1: The test engine specification

Engine Type	Single cylinder, 4-stroke
Total Displacement/Volume (V_t)	449.30 cc
Bore (B)	97 mm
Stroke (S)	60.8 mm
Compression Ratio (r_c)	12.5:1
Connecting Rod length (l)	107.40 mm

FE MODELLING METHODOLOGY

The methodology followed in this work is as the following. The finite element (FE) analyses were carried out using model 2 (Fig. 6) as described in [8].

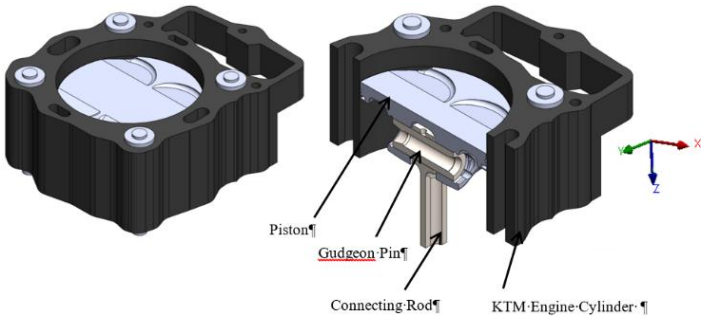

Figure 6: CAD assembly for the piston finite element analysis

To constrain the FE model; a node was fixed in the middle of the connecting rod's bottom face (Fig. 7a) and fixed supports were used on the bottom cylinder washers and studs to represent the cylinder being attached to the engine body (Fig. 7b). Furthermore, a pressure of 5.22 MPa was applied to the top washers (Fig. 7c) to represent the clamping force of 30 N that was applied to the studs/nuts on the cylinder.

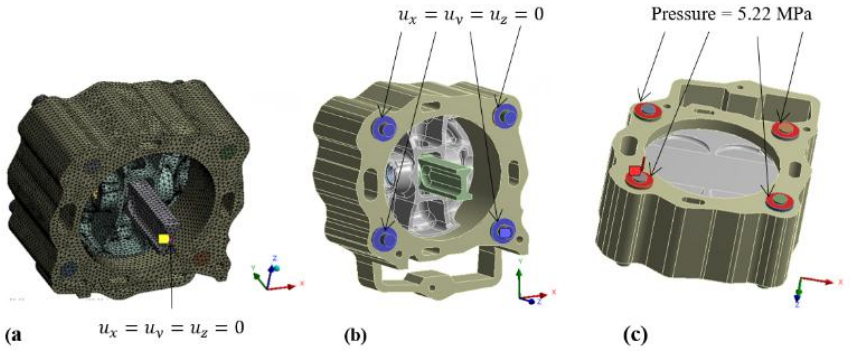

Figure 7: Application of the boundary conditions to FE model.

Eq. (1) was used to convert the torque into force (F) which was then converted into pressure using the surface area of the washers [16].

$$T = cDF \quad (1)$$

Where T, c, D and F are torque, coefficient of friction constant, nominal bolt diameter and F is the bolt tension (axial load).

The contacts between piston-pin, pin-connecting-rod and piston-cylinder were specified as frictional contacts which required the friction coefficient values to be specified. Determining the real friction coefficient values between these contacts was practically difficult. Other researchers such as [17] had tried to determine these coefficients, giving values that change with the engine speed. A constant value of 0.01 is used in this work which is also used in literature [18].

2.1. Material Properties

The FE model has numerous parts (a gudgeon pin, a connecting rod, a cylinder, cylinder mounting threaded studs, washers and a piston) [8] that are made of different materials. In the case of this test engine, the gudegeon pin and connecting rod is made of AISI 8620 steel, cylinder of A356 aluminium alloy, cylinder mounting threaded studs and washers of 316 stainless steel. The mechanical properties of these materials needed for piston FEA can be found from [19-23].

The original piston for the test engine is made of aluminium alloy 2618-T6 [24] and all the properties for alloy 2618 were taken from [21] while the Young Modulus values were taken from [20] (Table 2).

Table 2: Mechanical properties of the two piston alloys.

Property		Al-2618-T6	RSA-612-T6
Density, ρ (Kg/m^3)		2760	2550
Poisson Ratio, ν		0.33	0.33
Thermal Conductivity, k (W/m°C)		146	130
	Temperature (°C)		
Young's Modulus, E (GPa)	25	74	85
	100	72	82.5
	150	70	81
	200	68	79
	250	65	77.5
	300	61	75
	350	51	72.5
Ultimate Tensile Strength, σ_u (MPa)	25	441	424
	100	427	412.5
	150	345	394
	200	221	290
	250	90	117
	300	52	49
	350	34	28.5
Yield Strength, σ_y (MPa)	25	372	409
	100	372	391
	150	303	381
	200	179	279
	250	62	113
	300	31	48
	350	24	26
Coefficient of Thermal Expansion, CTE (µm/m.K)	25	20.6	18
	100	22.3	19.5
	200	23.2	20.2
	300	24.1	21

2.2. Determination of Loads

The mechanical and thermal loads acting on the piston were determined using the equations given in [8] and the results are given as the following.

2.2.1. Mechanical Loads

The engine used in this work was tested on dynamometer in its original configuration to obtain engine performance parameters such as in-cylinder pressure (Fig. 8), fuel consumption, air fuel ratio etc. The in-cylinder pressure sensor used was a spark plug integrated sensor from Optrand.

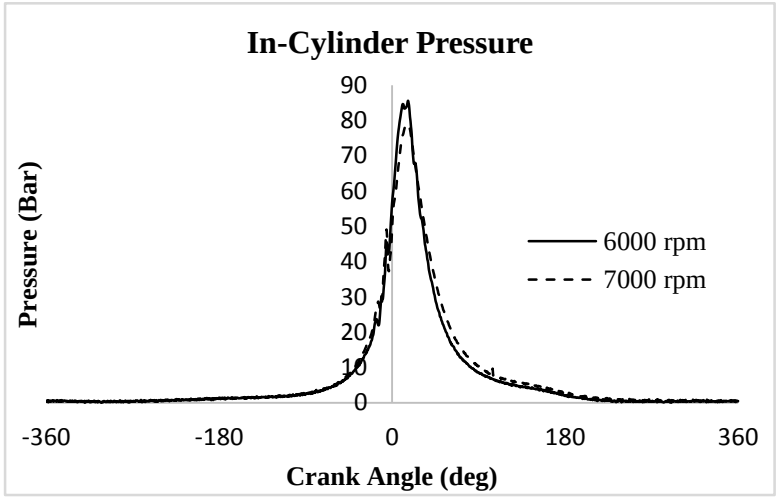

Figure 8: The in-cylinder pressure traces of the test engine at different engine speeds.

Determinations of inertial (Fig. 9) and lateral forces (Fig. 10) require mass of reciprocating components which was 455 grams in total and they are made of masses given in Table 3.

The piston's acceleration was determined using Eq. (2) from reference [8]

$$\ddot{x} = -r\omega^2(\cos\theta + \frac{r}{l}\cos 2\theta) \qquad (2)$$

Where $\ddot{x}$, r, ω, θ and l are the piston's acceleration, crank offset or crank radius, crank angular velocity, crank angle and the connecting rod length respectively.

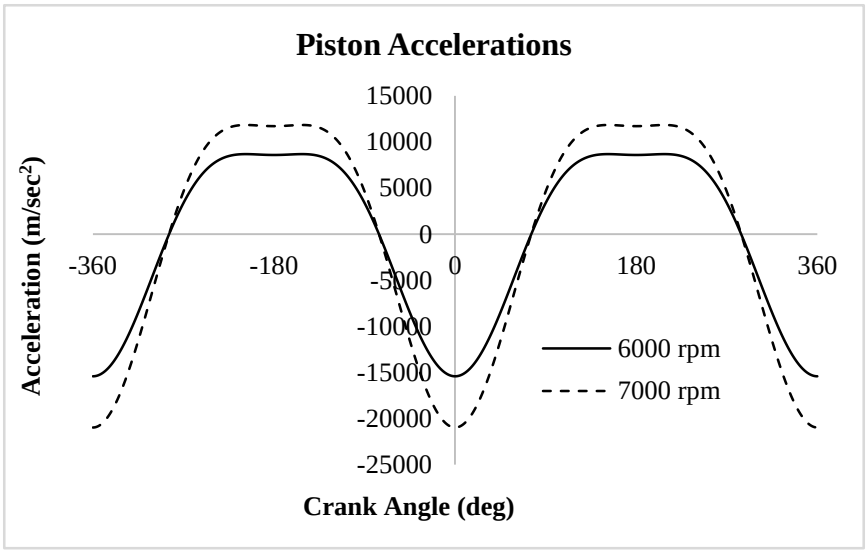

Figure 9: Piston accelerations of the test engine at different engine speeds.

Table 3. Masses of reciprocating components.

Component Name	Mass (g)
Piston	268.59
Pin	68.98
Circlip	0.84
Compression Ring	4.74
Oil Ring	6.44
Connecting Rod Small End	105.73
Total	455.32

The lateral force on the piston was determined using Eq. (3) from reference [8]

$$L_f(\theta) = -\left(m_B\ddot{x} + F_g\right)\tan\phi \qquad (3)$$

Where m_B is mass of the reciprocating components that include the piston, the pin and one-third of the connecting rod's mass. ϕ is the angle that the connecting rod makes with the cylinder axis.

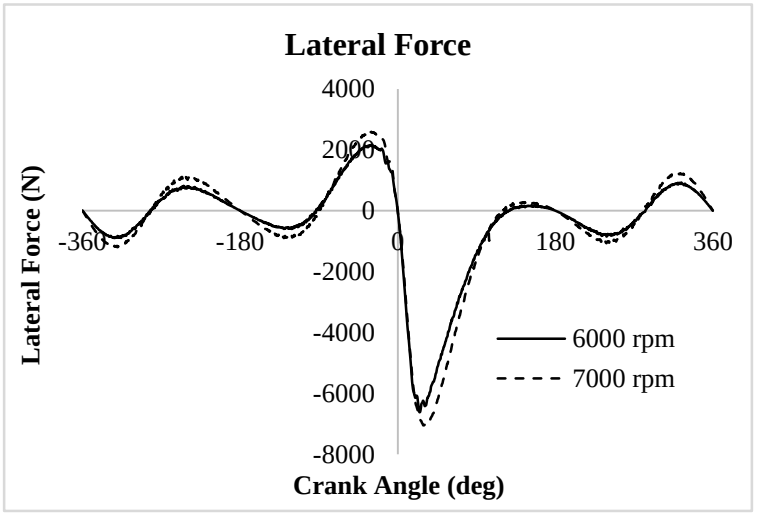

Figure 10: Lateral forces of the test engine at different engine speeds.

2.2.2. Thermal Loads

Having used various Eq. (6-22) from [8] to determine the combustion gas temperature the heat transfer between the piston and its surroundings was evaluated. The engine cooling oil properties and other relevant data, which were needed to determine the heat transfer coefficients at different piston regions, are given in Table 4. The heat transfer convention coefficients in different areas of the piston were determined and the results are given in Tables 5-6.

Table 4: Engine cooling oil properties and other relevant data [25]

Property	Value
Density	848 (kg/m^3)
Dynamic Viscosity	0.025 (kg/m.sec)
Thermal Conductivity	0.137 (W/m.K)
Specific Heat Capacity	2160 kJ/(Kg.K)
Engine Lubrication	10W50
Engine Oil Temperature	100 °C
Lubricating Oil Film (Piston-cylinder gap)	61 µm

Table 5: Heat transfer convention coefficients at different regions of piston

Heat Transfer Convection Coefficients	Value (W/m^2.K)	
	6000 rpm	7000 rpm
Combustion Gas and Piston Crown	475, 1012 °C	580, 904 °C
Ring Lands, Piston Outer Skirt and the Cooling Oil	4624, 100 °C	4624100 °C
Piston Under-Crown, Inner Skirt Walls and the Cooling Oil	1705, 100 °C	1929, 100 °C
Cylinder and Engine Cooling Jacket	1480, 100 °C	1480, 100 °C

Table 6: Heat transfer convention coefficients in compression ring of piston.

Property	Compression Ring Faces	
	Upper Face	Lower Face
Heat Transfer Coefficient (W/m^2.K)	885	1818
Temperature (K)	433	433

2.3. Critical Load Case

It can be deduced from Figs. 8-10 that the maximum values for different mechanical loads occurred at different angular positions of the crankshaft. In order to avoid neglecting any combination of these forces that might be critical, a number of appropriately selected points in time were analysed as suggested by [26]. The maximum combustion pressure load case that occurs at a crank angle of 16.5° after the top dead centre (TDC) for the analysed engine speed of 6000 rpm, turned out to be the most critical, causing the highest stress in piston. The results presented in this work therefore focused on this load case. The mechanical load values for the maximum combustion pressure load case at 6000 rpm are given in Table 7.

Table 7. Mechanical loads values in the maximum combustion load case at 6000 rpm.

Load	Value
Pressure	85.5 bar
Acceleration	14356 m/sec^2
Lateral Force	5626 N

Once a finite element model for the original piston was established, it was used as a base model to design a new piston with reduced mass by thinning the different sections of the piston.

2.4. Mass Reduction Strategy

For the new piston to be compatible with existing engine assembly there were certain features and sections of the piston that needed to be kept the same. These are highlighted in Fig. 11. Furthermore, the whole of the external envelope of the piston was also left unmodified to not affect the combustion characteristics of the engine.

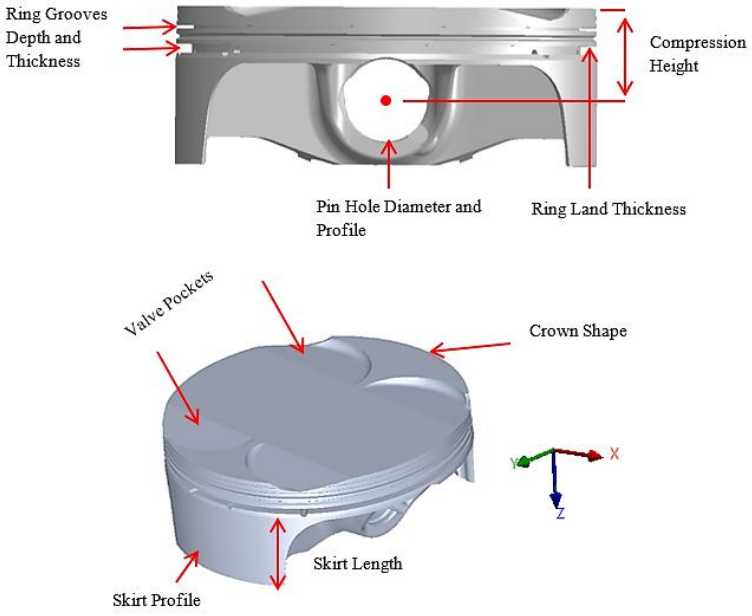

Figure 11: Features and regions of piston that we were left unmodified.

The design approach was to reduce piston mass by thinning different sections of the piston as stated earlier. This was feasible because the new alloy has higher strength and Young's Modulus (Table 2).

The inspection design optimisation was carried out by manually removing material from low stressed locations of the piston and re-evaluating stress and deformation response to verify acceptability. The parameters measured were the maximum principal stress, temperature and deformations and the simulated results are given in Figs. 12–24. The incremental material removal steps are tabulated in Table 8 which shows where the geometrical changes were made; resulting in material being removed. The simulation No in (Table 8) refers to each incremental step where the materials were removed for mass reduction.

RESULTS

The results presented in this section are based on the critical load condition (Table 7) and results are presented for piston temperature distribution, maximum principal stress, plastic strain and deformation. These values are significant factors in piston design analysis. A mesh convergence analysis was carried out which indicated that convergence occurred at an element size of 3.5 mm.

Most pistons fail due to thermo-mechanical fatigue loading where the crack starts at the high stress areas in crown above the pin hole (Fig. 12, circled in red) and travels towards the high stress area in pin hole (Fig. 13, shown in red). Therefore, the maximum principal stresses were assessed at critical locations that cause thermos-mechanical fatigue failures in piston as reported by [27-29]. The stress contours shown in Figs. 12-13 are for simulation No 1 (original design) and 16 (new final design) respectively. The directional Cartesian axes used for the analyses aligned with the pin longitudinal direction (X), radial to the pin longitudinal direction (Y) and the notional direction of the piston motion (Z), as shown in Fig. 6.

Table 8: Descriptions of the material removal steps for manual piston optimisation.

Simulation No	Piston Features	Original Dimension (mm, Degree)	New Dimensions (mm, Degree)	Mass (g)	% Mass Reduction from Original
1	Original Piston Design with Original Material			261.13	0
2	Original Piston Design with New Material Properties Only			241.26	7.61
3	Piston Crown	5.542 mm	5 mm	239.9	8.13
4	Piston Crown		4.5 mm	238.73	8.58
5	Ring Land Area	6.893 mm	6.5 mm	233.84	10.45
6	Ring Land Area		6 mm	225.13	13.79
7	Skirt Thickness	2.505&2.255 mm	2.3&2.1 mm	224.03	14.21
8	Undercrown Web Thickness			219.98	15.76
9	Web Fillets	5 Deg	3 Deg	218.62	16.28
10	Web Cut	33.302 mm	30 mm	215.4	17.51
11	Undercrown-Boss Fillets	5.2 mm	3 mm	215.04	17.65
12	Web-Boss Fillets	3.8&3 Deg	3&2.7 Deg	214.75	17.76
13	Undercrown-Skirt Fillet	6&5.5 mm	4&3.5 mm	212.11	18.77
14	UnderCrown-Boss-Skirt Fillets	3.5-3.2-3.5 Deg	2.8-2.6-2.80 Deg	211.49	19.00
15	Web-Skirt Fillets	5.1 & 2.9 Deg	3.5&2 Deg	210.48	19.39
16	Piston Crown	6 mm	6.2 mm	218.35	16.38

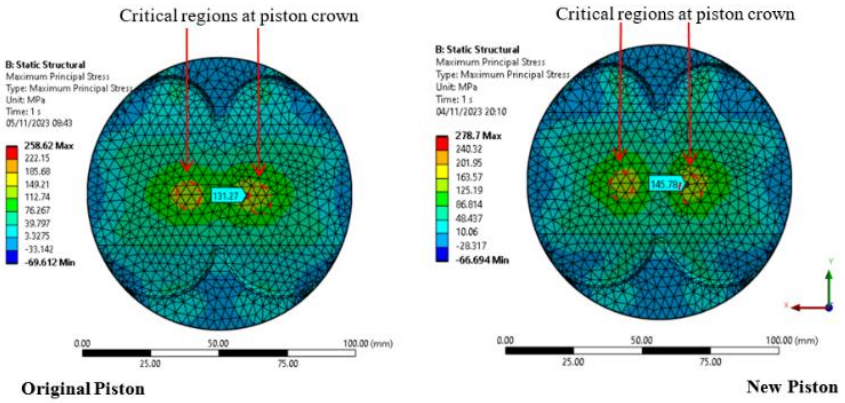

Figure 12: Maximum principal stresses in piston crown in original and new pistons.

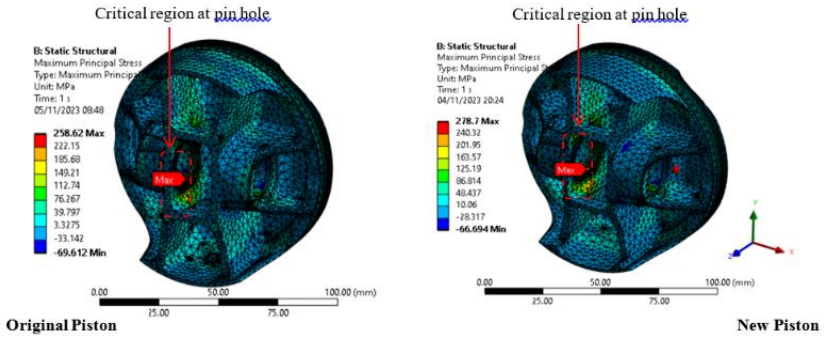

Figure 13: Maximum principal stresses in pin hole in original and new pistons.

1.1. Piston Design FEA Results

The maximum principal stresses in the critical regions (shown in Figs. 12-13) for the manual piston optimisation are given in Figs. 14–15.

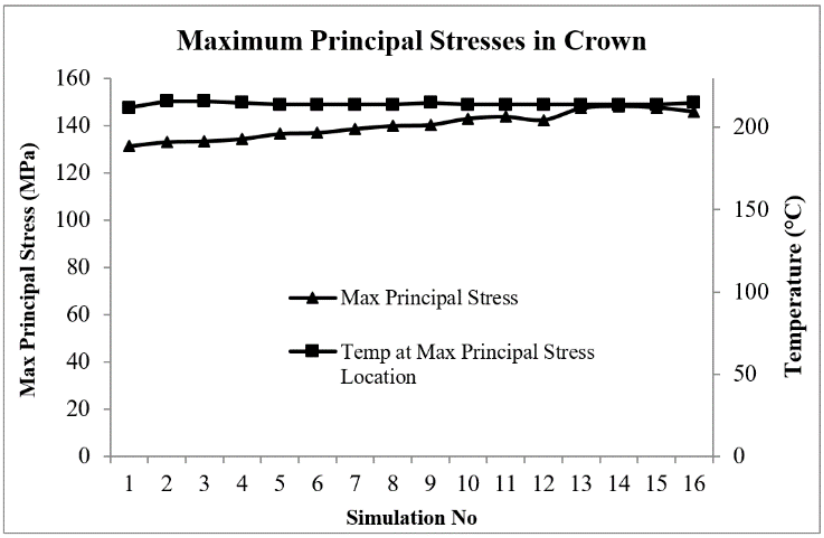

Figure 14: Maximum principal stresses in the piston crown due to incremental material removal.

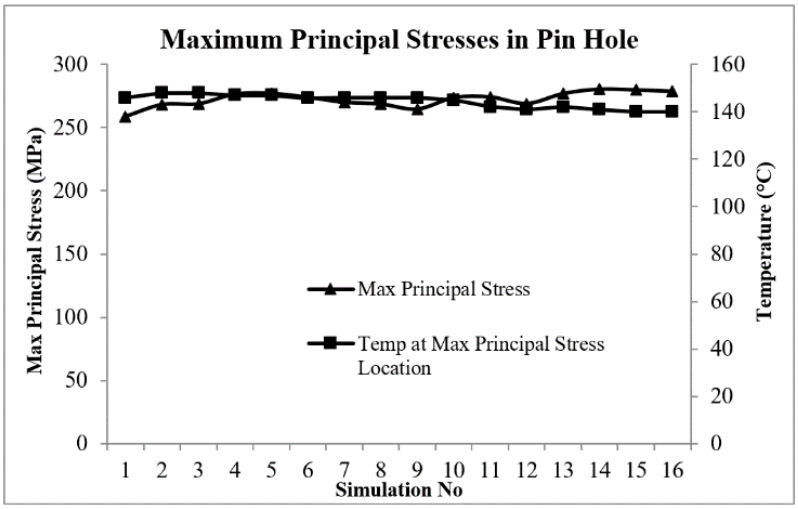

Figure 15: Maximum principal stresses in pin hole due to incremental material removal.

The temperature distribution contours in both original and new pistons are shown in Fig. 16. The maximum piston temperature and maximum deformations in X, Y and Z directions due to the incremental material removal can be seen in Figs. 17 and 18 respectably. The maximum temperature occurred at the locations (valve pocket edges) that were the furthest from any cooling surfaces.

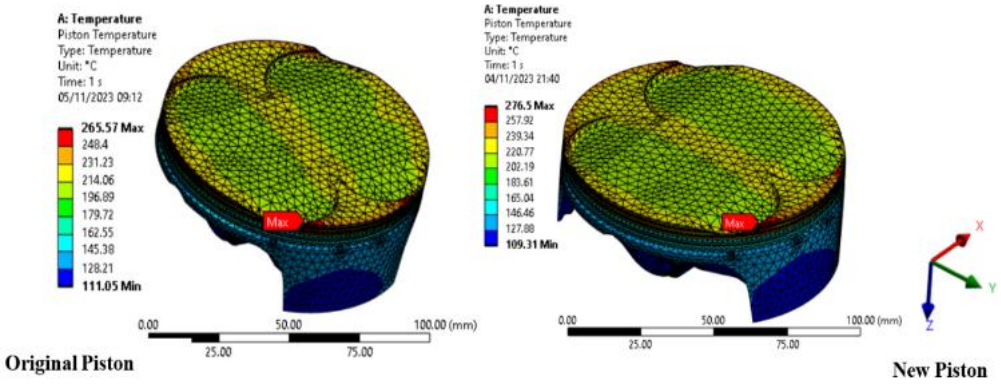

Figure 16: Piston temperature distributions in both original and new pistons

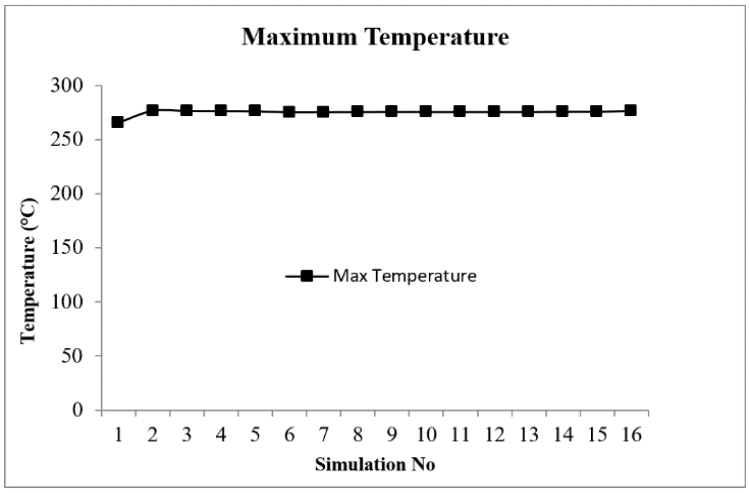

Figure 17: Maximum temperature changes in piston due to incremental material removal.

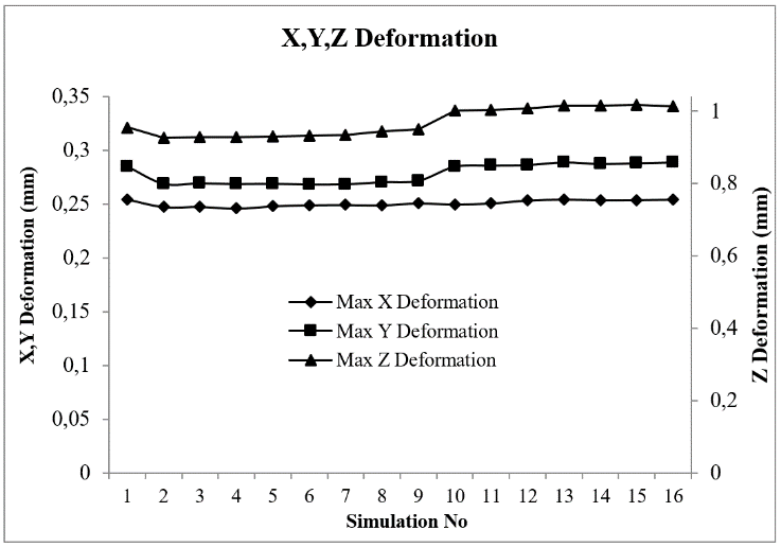

Figure 18: Maximum deformation changes in piston due to incremental material removal.

The comparison of the directional deformations of the optimised piston in X, Y and Z directions can be seen in Figs. 19–24. The measurements were taken on the piston crown on the red dashed line [8].

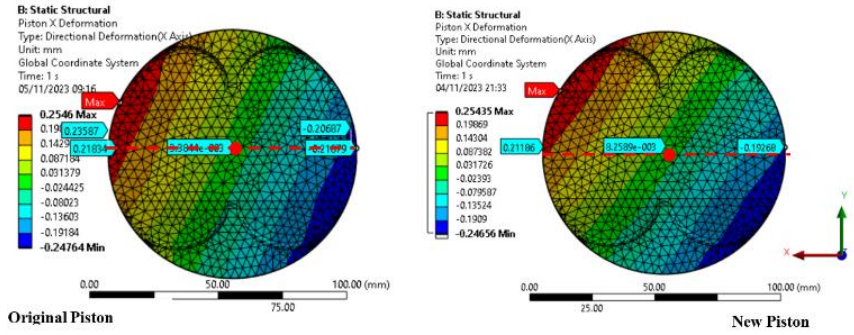

Figure 19: Piston deformation plots in X directions for both piston designs.

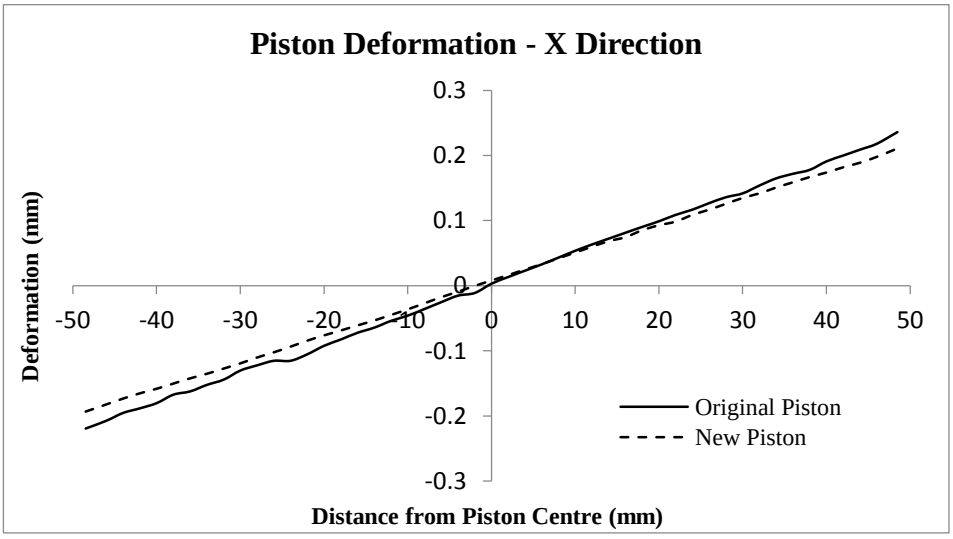

Figure 20: Piston deformation graphs in X directions for original and new pistons.

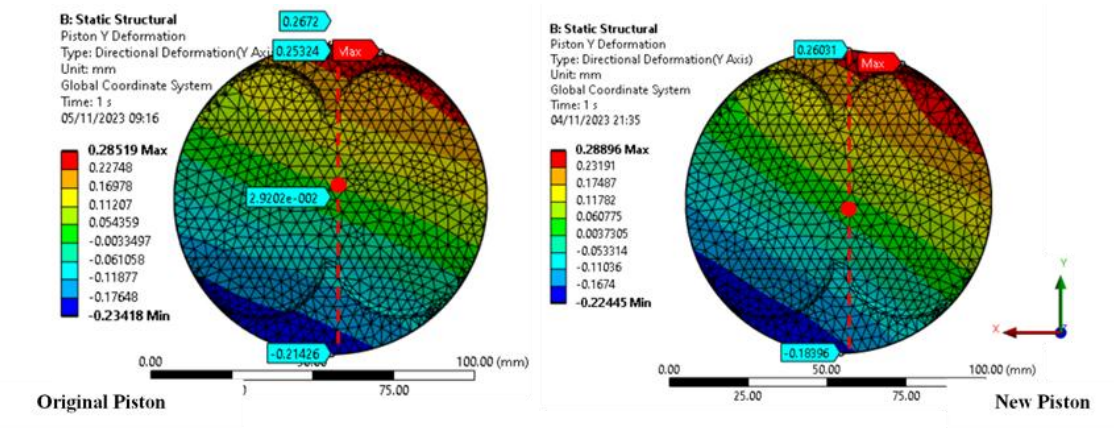

Figure 21: Piston deformation plots in Y directions for both piston designs.

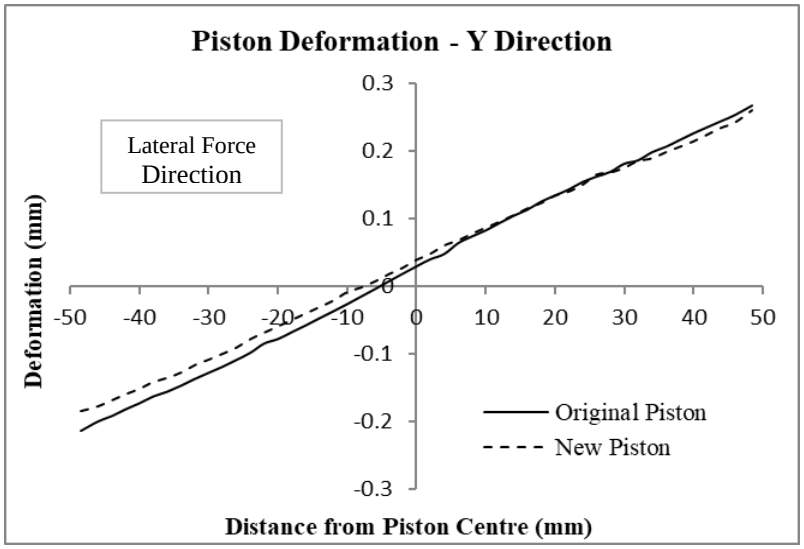

Figure 22: Piston deformation graphs in Y directions for original and new pistons.

Note: The lateral force direction is the same as the thrust side of the piston or in the direction of the intake valves. Pistons skirt on this side is designed thicker to resist the larger deformation caused by lateral force.

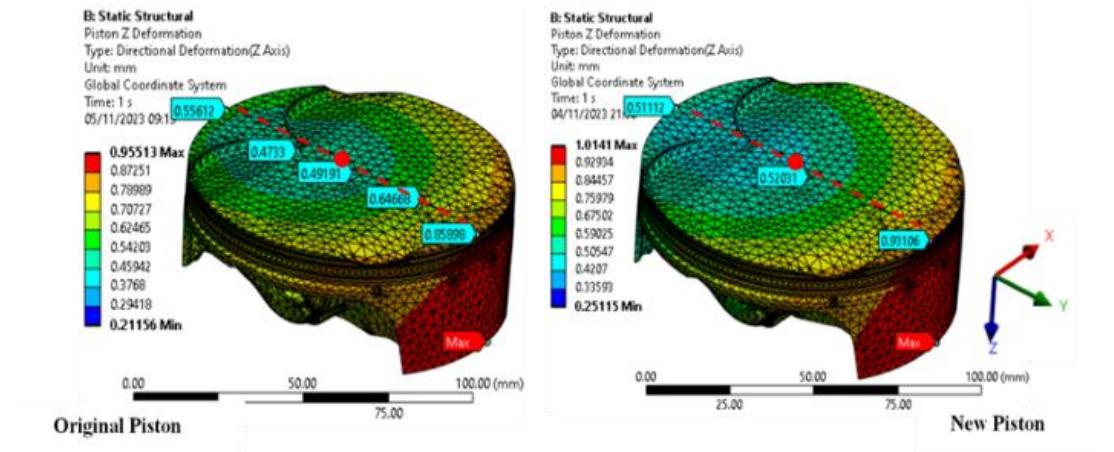

Figure 23: Piston deformation plots in Z directions for both piston designs.

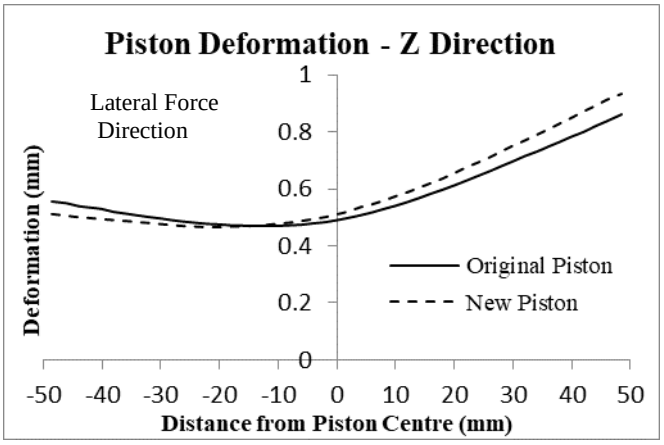

Figure 24: Piston deformation graphs in Z directions for original and new pistons.

A dimensional and feature comparison of the original and new pistons is illustrated in Fig. 25. The different features are highlighted/ numbered (in red) with respect to the simulation numbers in Table 8.

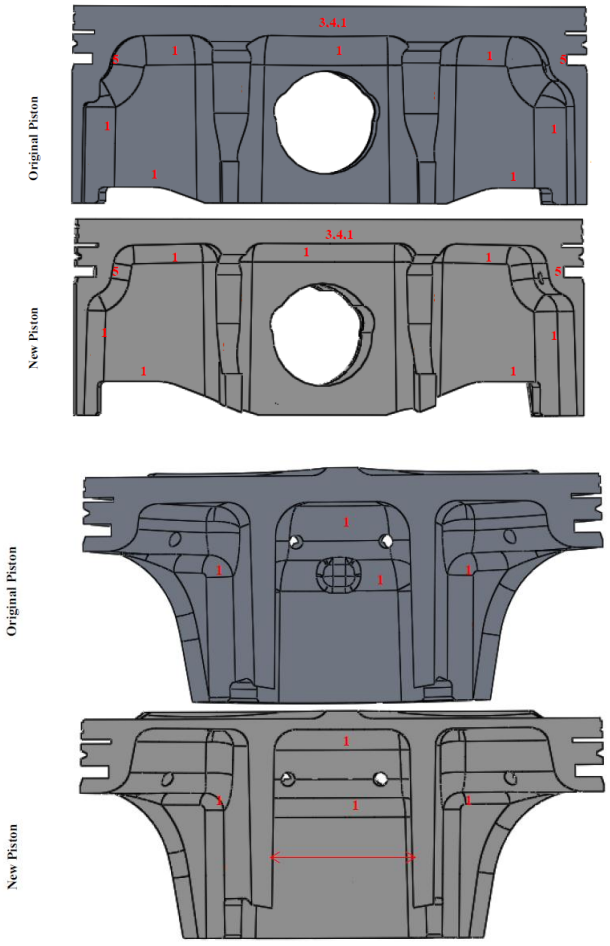

Figure 25: Comparison of original and new piston design.

3.2. Engine Test Results

The engine tests were carried out on dynamometer with the original and new pistons. The original piston was tested twice, where the purpose of the first tests was to obtain the worst case loading on the piston for designing the new piston. The engine was therefore tested at speeds of 3500, 4000, 5000, 6000 and 7000 rpm in half and full throttle positions. The critical load case occurred at 6000 rpm at full throttle (Table 7).

The second set of tests with the original piston was carried out at 3000, 4500 and 6000 rpm at different fixed torques ranging from 6-24 Nm at increment of 3 Nm. In the second case with the new piston, tests were

carried out at the same conditions as for the second set of the tests with the original piston. Measurements were taken under the same operating conditions in order to determine any gains or losses in the engine performance.

At each operating condition, the engine was allowed to run for about 5-6 minutes until it reached thermal stability in the new state before any measurements were taken. Thermal stability was established by monitoring the coolant temperature and the amount of exhaust oxygen (from lambda sensor readings) until they stopped fluctuating. Furthermore, it is impossible to keep the engine speed constant on dynamometer especially for a single cylinder engine, hence the effects of marginal speed fluctuations have been ignored.

The engine was tested in third gear only for all the engine speeds. The engine had a gear ratio of 3.32 between the gear box and output sprocket for third gear and the torque values obtained from the dyno were therefore divided by 3.32 to get the actual torque. The various performance indicators that were measured experimentally for both test configurations were fuel consumption, torque, intake pressure, test cell temperature, coolant temperature, air fuel ratio and in cylinder pressure. Other fundamental performance indicators such as mass flow rate of air, brake specific fuel consumption and volumetric efficiency were calculated using the values from experimental results. The engine performance results for both configurations in a graphical form are given in Figs. 26–27.

a)

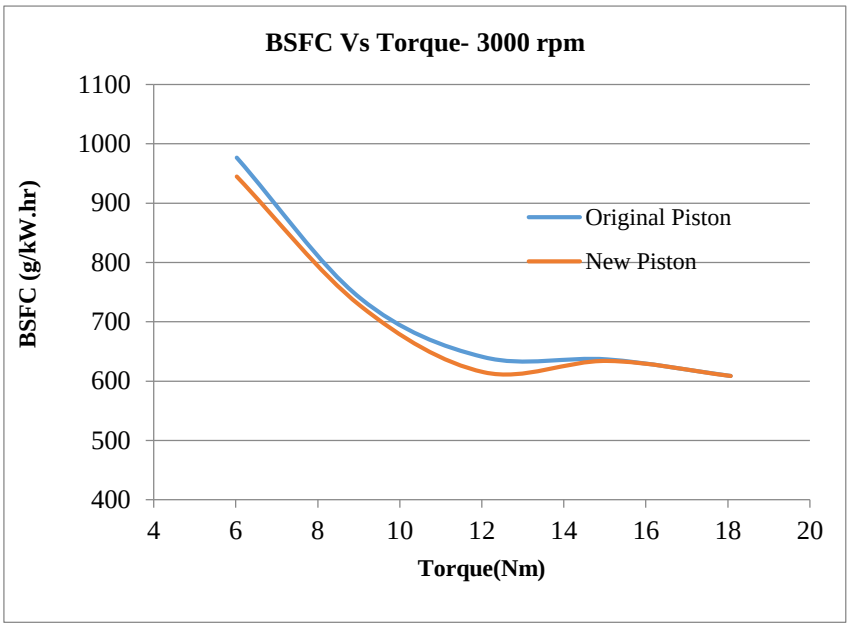

b)

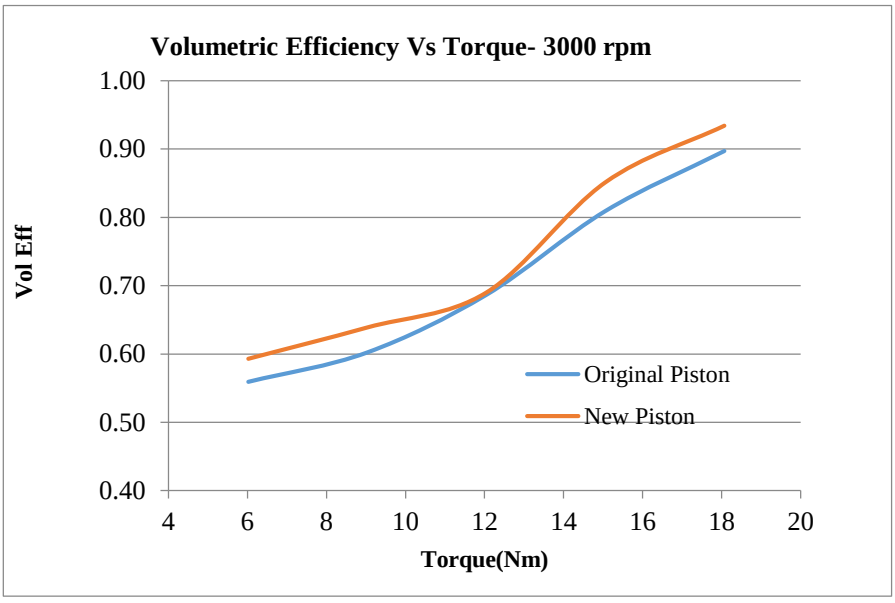

Figure 26: Comparisons of two performance indicators for original and new pistons at 3000 rpm a) Brake specific fuel consumption (BSFC) vs. torque b) volumetric efficiency vs. torque

a)

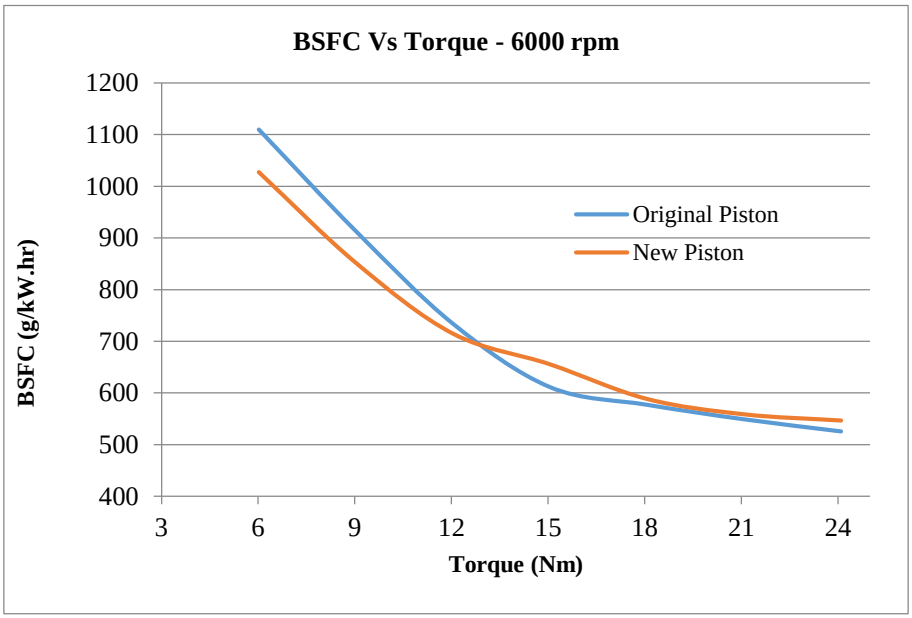

b)

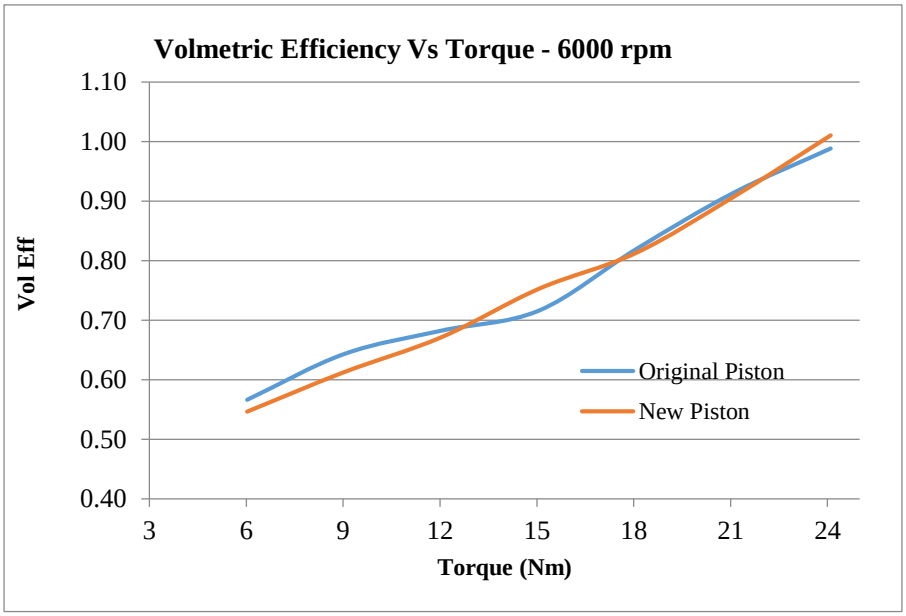

Figure 27: Comparisons of two performance indicators for original and new pistons at 6000 rpm a) BSFC vs. torque b) volumetric efficiency vs. torque

The test results in Figs. 26-27 clearly show improvements in the engine performance in terms of torque and fuel consumption. However, more detailed discussion of these results is presented in Section 4.2.

DISCUSSION

4.1. Finite Element Analysis of New Piston and Implementation of the new piston in the engine with existing components

In order for the new piston to be compatible with the existing engine components, the new piston had to be designed with a number of constraints (See Section 2.4). These constraints made it more challenging to reduce the mass as many sections of the piston could not be modified (Fig. 11). One of the two approaches used to reduce the piston mass was topology optimisation, but it was too limited for application in this project. However, some adjustments were made to see if it will work. Despite, these adjustments the results were not of

any practical use hence it was decided to use an iterative/inspection approach to reduce the piston mass using the FEA Model 2 [8].

The different iterations carried out are tabulated in Table 8 and it can be seen that the piston mass determined from computer aided design (CAD) was reduced by 16.38% without increasing the stresses significantly as indicated in Figs. 12–15. The small increase in stress is not of any concern since the new alloy has higher strengths at elevated temperatures than the original alloy (Al-2618, see Figs. 3-4). Furthermore, the directional deformations of the new piston design stayed nearly the same as the original piston (Figs. 19–24).

The actual machined piston turned out to be slightly heavier than the final optimised piston model, it was due the coating and also some modifications needed to make the design machinable. However, the final machined piston was still 13.5% lighter than the original piston.

4.2. Engine Test Results of Original and New Pistons

The results for 3000 rpm in Fig. 26 indicated that the new piston was more fuel efficient compared to the original piston especially at lower torque (Figs. 26a-b). This may be attributed to the higher volumetric efficiency of the engine which leads to leaner operation of the engine with the new piston (Figs. 26b). The air fuel ratio (AFR) values measured were higher / leaner for the new piston compared to the original piston. For the same torque, the engine with higher volumetric efficiency will consume less fuel due to the availability of more Oxygen which reduces ignition delay hence converts more of the fuel energy to useful work [30]. Furthermore, higher volumetric efficiency in general is considered a desirable characteristic because it leads to higher power output and improves specific fuel consumption [31-34]. However, it can affect the factors that reduce pumping work/losses (the work in exhaust and intake strokes). The increased power output can lead to higher exhaust flow rates during the exhaust stroke, which can in turn increase the work required to expel the exhaust gases due to increased backpressure and frictional losses [35].

The results for engine speed of 6000 rpm showed that the new piston was more fuel efficient than the original piston at lower torque and mass flow rate of air (MFRair) values of less than 13 Nm or 235 g/sec respectively (Figs. 27a-b). The engine with both pistons had nearly the same volumetric efficiencies (Figs. 27b). The lower fuel efficiency of new piston at certain torque values despite similar volumetric efficiency especially at higher torque values may be due to the higher intake air temperature which adversely affect engine performance due to decrease in Oxygen availability.

Many researchers [30, 32-34] have investigated the impact of intake air temperature on engine performance specifically fuel consumption and all reported that decreasing air intake temperature decreases fuel consumption due to the increasing amount of Oxygen in air. Colder air has higher Oxygen density compared to hotter air. In addition; lower air intake temperature reduces ignition delay and the combustion starts at the end of the compression stroke and early expansion stroke therefore converts larger portion of the fuel energy to useful work.

Furthermore, the research by [30] showed that the impact of air intake temperature on engine performance is more dominant at higher engine speeds. This is due to the higher injected fuel at higher engine speed which requires more Oxygen to complete the combustion. Birtok-Baneasa, 2017 [30] demonstrated that a 10 degrees increase in air intake temperature from 20 °C to 30 °C resulted in 4% more fuel consumption at 1500 rpm while this value increased to 22 % at engine speed of 3000 rpm.

Also, the test engine in this project was using carburettor not fuel injector which most modern engine use and therefore the air fuel mixture could not be controlled.

Even though testing of the new piston has demonstrated application of the new alloy in higher temperature applications such as pistons for internal combustion engine. However, the engine testing facility available for this research was not able to control certain parameters that could affect the engine performance such as air-intake temperature, humidity etc. The test cell temperature was measured during testing, but it could not be controlled. On average the test cell temperature was 6 °C higher for new piston than the original piston and this would have negatively impacted the engine performance. The test cell was drawing air directly from the outside environment and the air temperature could not be controlled. Due to the availability of the test cell, the new piston was tested in summer while the original piston was tested in winter which resulted in the different test cell temperatures for the two set of engine tests.

The limited engine testing results presented in this work have shown that the new piston produces enhanced performance in certain operating conditions, whilst performing similarly or slightly worse in others. To ultimately determine whether the new lightweight piston would generate any sizeable difference in engine performance and/or efficiency across the wider engine running envelope, further work is needed.

CONCLUSION

The application of a newly developed aluminium based nanostructured alloy in pistons was assessed in this work to evaluate the potential mass reduction of the piston under consideration. The new piston's mass determined from computer aided design (CAD) was 218.35 grams which was 16.38% lighter than the original piston with mass of 261.13 grams. The actual machined piston turned out to be slightly heavier than the final optimised piston design. This was due to the coating and some modifications needed to make the design machinable. However, the final machined piston was still 13.5% lighter than the original piston.

It could not be conclusively said from the results if the new piston was more fuel efficient overall in all test conditions, but the new piston was more fuel efficient than the original piston at higher speeds and lower torques. At lower speed of 3000 rpm, the new piston was more fuel efficient in all torque values. Overall, the new piston has higher volumetric efficiency compared to the original piston, but at higher engine speed of 6000 rpm and higher torque the new piston had lower volumetric efficiency.

The research also highlighted the limitations such as controlling test cell temperature, humidity etc. in the engine test facility available for the research, which would have negatively affected the engine performance. The test cell temperature, which was also the temperature of the intake air, was 6 °C higher on average for the new piston which would have adversely impacted engine performance with the new piston.

Further work is advised to ultimately determine if the new alloy gives any significant performance gains.

ACKNOWLEDGEMENTS

The authors would like to thank RSP Technology for the provision of material and certain material properties as highlighted in the work.

CONFLICT OF INTEREST STATEMENT

All authors declare that we have no conflicts of interest

REFERENCES

[1] Blackmore DR. Fuel economy of the gasoline engine: fuel, lubricant and other effects. Springer; 1977 Jun 17.
[2] Merkle A, Kunkel S, Wachtmeister G. Analysis of the Mixed Friction in the Piston Assembly of a SI Engine. SAE International Journal of Engines. 2012 Aug 1;5(3):1487-97.
[3] Kohashi, K.-i. et al. (2013) 'Analysis of Piston Friction in Internal Combustion Engine', SAE Int. J. Fuels Lubr., 6(3), pp. 589-593. Available at: https://doi.org/10.4271/2013-01-2515.
[4] Schwaderlapp M, Dohmen DI. Friction reduction-the engine's mechanical contribution to saving fuel. SAE Technical Paper; 2000 Jun 12.
[5] Nagar P, Miers S. Friction between Piston and Cylinder of an IC Engine: a Review.
[6] Agarwal VK. Effect of Design and Operational Parameters of Piston Skirt on the Performance and Efficiency of a Small Gasoline Engine. SAE Technical Paper; 2014 Mar 24.
[7] Norton, R. L. (2012) Design of machinery: an introduction to the synthesis and analysis of mechanisms and machines, Fifth edition. New York: McGraw-Hill Higher Education.
[8] Adil H, Gerguri S, Durodola J, Fellows N, Bonatesta F, Audebert FE. Comparative Study and Evaluation of Two Different Finite Element Models for Piston Design.
[9] Winship, J. W. (1967) 'Designing an Automotive Engine Piston': SAE International
[10] Agarwal VK. Effect of Design and Operational Parameters of Piston Skirt on the Performance and Efficiency of a Small Gasoline Engine. SAE Technical Paper; 2014 Mar 24.
[11] Goenka PK, Meernik PR. Lubrication analysis of piston skirts. SAE transactions. 1992 Jan 1:886-95.
[12] Adil H, Gerguri S, Durodola J, Audebert F, Bonatesta F, Saporiti F. Evolution of Materials for Internal Combustion Engines Pistons.
[13] Smith MT, Richland WA. High-Temperature Aluminum Alloys. Pacific Northwest National Laboratory. 2012 May 15.
[14] Adil H, Audebert F, Saporiti F, Gerguri S, Bonatesta F, Durodola J. F. Microstructure and Mechanical Properties of an Al-Mg-Si-Cu Alloy for High Temperature Applications. Mat. Sci. Res. India;20(3). Available from: https://bit.ly/3Qd1I0d
[15] GmbH, M. (2016) Pistons and engine testing, Second edition. Heidelberg: Springer Vieweg. ATZ/MTZ-Fachbuch.
[16] Edge, E. (2018a) *Coefficient of Friction Equation and Table Chart.* Georgia: Engineers Edge Available at: https://www.engineersedge.com/coeffients_of_friction.htm (Accessed: 05/06/2018).
[17] Schneider C, Halbhuber J, Wachtmeister G. Measuring and Simulating Friction between Piston Pin and Connecting Rod on a Tribometer Test Bench to Define Locally Resolved Friction Coefficients. SAE Technical Paper; 2016 Apr 5.
[18] Carvalheira P, Gonçalves P. Fea of two engine pistons made of aluminium cast alloy A390 and ductile iron 65-45-12 under service conditions. In5th International Conference on Mechanics and Materials in Design Porto-Portugal 2006 Jul (pp. 24-26).

[19] Bardes, B. P. and American Society for Metals. Handbook, C. (1978) Metals handbook. Vol.1, Properties and selection: irons and steels, 9th. ed. Metals Park, Ohio: American Society for Metals.
[20] Kaufman JG, editor. Properties of aluminum alloys: tensile, creep, and fatigue data at high and low temperatures. ASM international; 1999.
[21] Bray JW. Properties and selection: Nonferrous alloys and special purpose materials. ASM Metals handbook. 1990;92.
[22] SSINA (2009) High Temperature Properties. USA: The Stainless Steel Information Centre Available at: http://www.ssina.com/composition/temperature.html (Accessed: 08/07/2018).
[23] Harvey PD. Engineering properties of steel: Metals Park. Ohio, ASM. 1982.
[24] VertexPistons (2018) Vertex Piston Kits. USA: Vertex Pistons Inc. Available at: http://www.na.vertexpistons.com/ProductInfo.aspx?cat_details_id=31 (Accessed: 02/12/2018).
[25] Thermal-FluidsCentral (2011) 'Thermo-Physical Properties: Engine Oil, Unused'. Available at: https://www.thermalfluidscentral.org/encyclopedia/index.php/Thermophysical_Properties:_Engine_Oil,_Unused (Accessed 07/03/2017).
[26] Mahle, G. (2016) Pistons and engine testing, Second edition. Heidelberg: Springer Vieweg. ATZ/MTZ-Fachbuch.
[27] Silva FS. Fatigue on engine pistons–A compendium of case studies. Engineering failure analysis. 2006 Apr 1;13(3):480-92.
[28] Floweday G, Petrov S, Tait RB, Press J. Thermo-mechanical fatigue damage and failure of modern high performance diesel pistons. Engineering Failure Analysis. 2011 Oct 1;18(7):1664-74.
[29] Dileep M, Sanjay PS, Mandloi RK. Analytical study of fatigue failure of aluminium alloy piston in IC engines. Inter Res Jour of Eng and Tech. 2016;3:1665-9.
[30] Birtok-Băneasă C, Raţiu S, Hepuţ T. Influence of intake air temperature on internal combustion engine operation. InIOP Conference Series: Materials Science and Engineering 2017 (Vol. 163, No. 1, p. 012039). IOP Publishing.
[31] Sher E. Handbook of air pollution from internal combustion engines: pollutant formation and control. Academic Press; 1998 Mar 20.
[32] Treeamnuk, T., Treeamnuk, K. and Papakae, S. (2018) 'Influence of Intake Air Temperature on Performance of Small Gasoline Engine', The Asian Conference on Sustainability, Energy & the Environment 2018. Thailand: The International Acadeic Forum, pp. 9.
[33] Khaifullizan MN, Jaat N, Abidin SF, Darlis N, Zahari I. Effect of Intake Air Temperature on Engine Performance and Fuel Consumption of Passenger Car. Fuel, Mixture Formation and Combustion Process. 2021 Aug 26;3(2).
[34] Pan W, Yao C, Han G, Wei H, Wang Q. The impact of intake air temperature on performance and exhaust emissions of a diesel methanol dual fuel engine. Fuel. 2015 Dec 15;162:101-10.
[35] TUNÇEL AL, AKYUZ E, ARSLAN Ö. © Copyright 2021 by the Journal of ETA Maritime Science published by UCTEA Chamber of Marine Engineers 210 An Extended Event Tree Risk Analysis Under Fuzzy Logic Environment: The Case of Fire in Ship Engine Room. Journal of Eta Maritime Science. 2021;9(3):210-20.